SAND REPORT

SAND2002-3954
Unlimited Release
Printed December 2002
Reprinted January 2003

MEMS Adaptive Optics Devices: LDRD No. 02-1385 Summary Report

Daryl J. Dagel, James J. Allen, Jeffrey L. Dohner, Kent B. Pfeifer, Michael B. Sinclair, Olga Blum Spahn, Christine M. Wehlburg, and Joseph C. Wehlburg

Prepared by
Sandia National Laboratories
Albuquerque, New Mexico 87185 and Livermore, California 94550

Sandia is a multiprogram laboratory operated by Sandia Corporation,
a Lockheed Martin Company, for the United States Department of
Energy under Contract DE-AC04-94AL85000.

Approved for public release; further dissemination unlimited.

Issued by Sandia National Laboratories, operated for the United States Department of Energy by Sandia Corporation.

NOTICE: This report was prepared as an account of work sponsored by an agency of the United States Government. Neither the United States Government, nor any agency thereof, nor any of their employees, nor any of their contractors, subcontractors, or their employees, make any warranty, express or implied, or assume any legal liability or responsibility for the accuracy, completeness, or usefulness of any information, apparatus, product, or process disclosed, or represent that its use would not infringe privately owned rights. Reference herein to any specific commercial product, process, or service by trade name, trademark, manufacturer, or otherwise, does not necessarily constitute or imply its endorsement, recommendation, or favoring by the United States Government, any agency thereof, or any of their contractors or subcontractors. The views and opinions expressed herein do not necessarily state or reflect those of the United States Government, any agency thereof, or any of their contractors.

Printed in the United States of America. This report has been reproduced directly from the best available copy.

Available to DOE and DOE contractors from
U.S. Department of Energy
Office of Scientific and Technical Information
P.O. Box 62
Oak Ridge, TN 37831

Telephone: (865)576-8401
Facsimile: (865)576-5728
E-Mail: reports@adonis.osti.gov
Online ordering: http://www.doe.gov/bridge

Available to the public from
U.S. Department of Commerce
National Technical Information Service
5285 Port Royal Rd
Springfield, VA 22161

Telephone: (800)553-6847
Facsimile: (703)605-6900
E-Mail: orders@ntis.fedworld.gov
Online order: http://www.ntis.gov/help/ordermethods.asp?loc=7-4-0#online

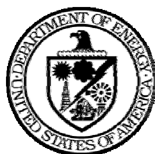

SAND2002-3954
Unlimited Release
Printed December 2002
Reprinted January 2003

MEMS Adaptive Optics Devices: LDRD No. 02-1385 Summary Report

Daryl J. Dagel, James J. Allen, and Jeffrey L. Dohner
MEMS Device Technologies

Kent B. Pfeifer
Microsensors Science and Technology

Michael B. Sinclair
Microsystems Materials, Tribology and Technologies

Olga Blum Spahn
RF Microsystems Technologies

Christine M. Wehlburg
Chemical and Biological Sensing, Imaging and Analysis

Joseph C. Wehlburg
Remote Sensing and Exploitation

Sandia National Laboratories
P.O. Box 5800
Albuquerque, NM 87185-1080

Abstract

This LDRD leverages the surface micromachining capability embodied in Sandia's Ultra-planar Multi-level MEMS Technology (SUMMiT™) to develop optical mirror arrays for spectroscopic remote sensing systems. The research consists of two parts: (1) the development of a programmable diffraction grating for use in a correlation spectrometer, and (2) the development of a programmable mask for use in a hyperspectral imager. From a design perspective, these efforts overlap considerably in terms of array geometry, layout, and optical tolerances and differ mainly with regard to the degrees of freedom of the mirror elements. Similarities exist on a functional level as well: both devices select a subset of the source spectrum for analysis. The first device, referred to as the Polychromator, reproduces the characteristic spectra of substances by changing the diffraction pattern reflected from its mirror array, while the second device, the Hadamard Transform Spectral Imager (HTSI), identifies the spectra of objects by sampling the different wavelength bands generated by a conventional grating.

Intentionally Left Blank

Acknowledgements

Thanks to Alex Pimentel for FIB analysis, Fawn Gass for finite-element modeling, Jeremy Walraven for failure analysis, Sita Mani for input on fabrication issues, and John Nevers for insight on electrical design. Thanks also to Ken Pohl, Mark Jenkins, and Grant Grossetete for help with characterization and high-speed photography. In addition, we thank the SAMPLES™ team for fabricating the SUMMiT™ devices.

Intentionally Left Blank

Table of Contents

Abstract………………………………………………………………………………….. 3
Acknowledgements………………………………………………………………………… 5
Table of Contents……………………………………………………………………….... 7
Part I…………………………………………………………………………………….... 8
Part II……………………………………….…………………………………………….. 20
Distribution List………………………………………………………………………….. 31

PART I

SUMMiT™ Vertical Programmable Diffraction Grating

James J. Allen and Jeffrey L. Dohner
MEMS Device Technologies

Michael B. Sinclair
Microsystem Materials, Tribology and Technologies

Kent B. Pfeifer
Microsensors Science and Technology

Sandia National Laboratories
P.O. Box 5800
Albuquerque, NM 87185

Abstract

The primary goal of this portion of the LDRD is to develop a vertical programmable diffraction grating that can be fabricated with Sandia's Ultra-planar Multi-level MEMS Technology, the SUMMiT V™ process. This grating is targeted for use in a chemical detection system dubbed the Polychromator. A secondary goal is to design diffraction grating structures with additional degrees of freedom (DOF). Gratings with 2.5 microns of vertical stroke have been realized. In addition, rotational DOF grating structures have been successfully actuated, and a structure has been developed that minimizes residual stress effects.

Table of Contents

Abstract……………………………………………………………………………………….. 8
Table of Contents……………………………………………………………………………... 9
List of Figures………………………………………………………………………………… 9
Background—The Polychromator…………….……………………………………………… 10
Design Concepts……………..………………………………………………………………. 11
Paved Design..………………………………………………………………………….. 11
Compound Leveraged Beam Bending Pull Down Device – "Toadstool"……………….11
Push-Up Programmable Grating Design…………………………………………….. 16
Rotational Programmable Gratings…………………………………………………… 17
Conclusions…………………..…………………………………………………………….. 18
References……………………………………………………………………………………… 19

List of Figures

Figure 1: Spectrum Modulated by a Tunable Diffraction Grating……………………………... 10
Figure 2: Schematic Representation of Leveraged Beam Bending…………………………….. 12
Figure 3: Schematic of Compound Beam Leveraged Bending Operation……..…...………… 12
Figure 4: SUMMiT™ Implementation of the Leveraged Bending Design……………………. 13
Figure 5: Side View of the "Toadstool" Segmented Programmable Grating………....…..…… 13
Figure 6: Isotropic View of the "Toadstool" Segmented Programmable Grating…….…..…… 14
Figure 7: Exploded View of the "Toadstool" Segmented Programmable Grating…….……… 14
Figure 8: SUMMiT V™ Variable Programmable Grating Test Array...………………………. 15
Figure 9: Voltage vs. Deflection of MMPoly4 Mirror in the "Toadstool" Design...…………... 15
Figure 10: Schematic of the Push-Up Programmable Grating Design…………………………. 16
Figure 11: 3-D Model of the Push-Up Design……………………………………………….. 16
Figure 12: Detailed View of the Actuating Beam and Joints in the Push-Up Design…...……... 17
Figure 13: Solid Model of Rotational Programmable Grating...……………………………….. 17
Figure 14: SUMMiT™ Rotational Programmable Grating…….………………………………. 18

Background – The Polychromator

Correlation spectroscopy is a valuable tool for sensing and analysis applications in which the optical transmission is determined and correlated over a fixed spectral range for an unknown sample with a reference cell containing the material of interest. The technique can be used for remote chemical sensing, but the reference cell will need to contain a sample of the material, which would make this device bulky and potentially hazardous, depending on the material to be analyzed. The realization that MEMS programmable diffraction gratings could be used to produce synthetic spectra of the material of interest was a breakthrough [1], and eliminates the need for a reference cell (Figure 1). This development also eliminates the need to have a multitude of reference cells for different materials, since the MEMS programmable grating can artificially synthesize the reference spectra for a multitude of materials on demand. The MEMS programmable diffraction grating is a large array of long, narrow optically reflective elements whose vertical positions are electrically controlled. The element length is many optical wavelengths, the width a few optical wavelengths, and the vertical positions controllable to a fraction of a wavelength.

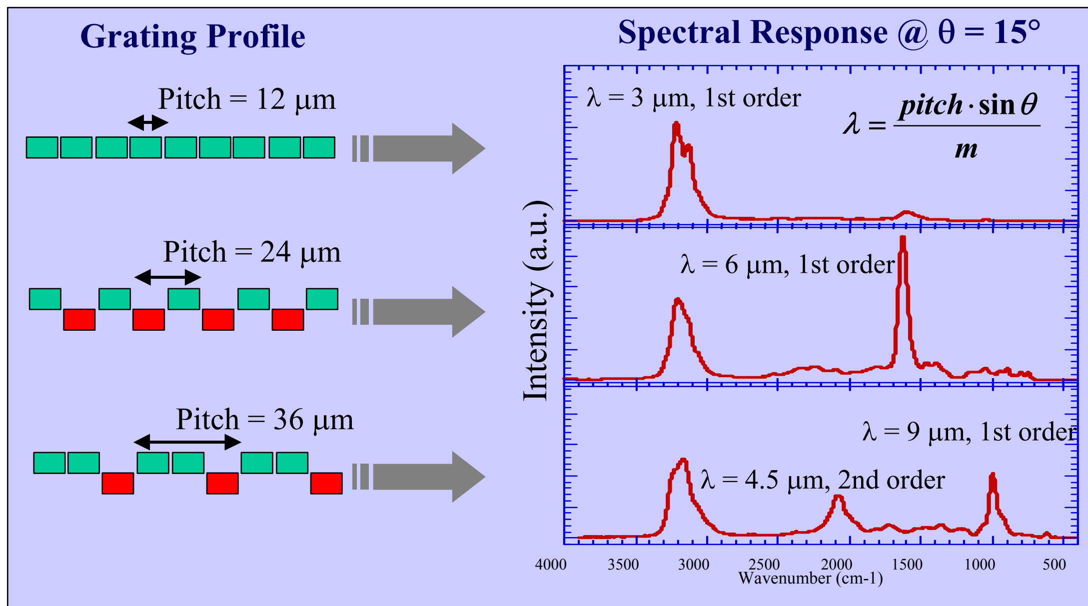

Figure 1: Spectrum Modulated by a Tunable Diffraction Grating.

The development of advanced programmable MEMS-based (SUMMiT™) diffraction gratings will lead to enhanced performance for existing systems such as the Polychromator, as well as enable new optical devices. Due to atmospheric transmission considerations, the 8-12 micron wavelength range is optimal for infrared chemical sensing. In addition, this spectral band often contains the chemical "fingerprint" bands that help to uniquely determine chemical species. However, operation of a diffractive MEMS device in this wavelength range requires relatively large beam displacements of approximately 6 microns in order to achieve the required 2π phase shifts. Thus, *the primary goal of this project is to develop electromechanical structures that*

successfully implement the large displacement actuation that is possible within the SUMMIT-V™ process.

The design of these types of structures presents a significant design challenge on a number of fronts, such as

- Large vertical deflection of a very narrow (20 micron wide) device within a MEMS fabrication process where the total height of all layers is 13 microns.
- The electrostatic-structural instability is at a fraction of the available electrostatic gap.
- Residual stress effects on the un-actuated and actuated structures must be minimized.
- Large arrays of these devices will be required in the application.

Design Concepts

Paved Design

The design of a continuous structure that is paved across the die was initially considered and test devices were fabricated. The SUMMiT™ fabrication process has a small compressive residual stress, but when trying to fabricate long structures (>500 microns) with multiple anchor points buckling and significant out of plane deflections are the unacceptable result. The design approaches that can mitigate these effects are:

- Segmentation of the device: Instead of a very long continuous structure, the approach of designing a small device, which mitigates buckling, can be utilized and then paved across the structure to mimic a long programmable diffraction grating.
- Minimization of anchors within the structure: The best way to minimize residual stress effects is to minimize the "anchors" within the device (i.e. support of the mirrored surfaces via a single point would be optimal)

Compound Leveraged Beam Bending Pull Down Device – "Toadstool"

This design approach incorporates the concept of leveraged beam bending [2] to mitigate the effect of electrostatic-structural instability. For a ideal lumped parameter realization of a spring supported electrostatic gap, it can be theoretically shown that the electrostatic-structural system will become unstable at 1/3 of the initial gap, regardless of the stiffness of the restraining spring. For more general structural systems incorporating an electrostatic gap for actuation this effect is also present at a fraction of the available gap. This would seemingly greatly limit the available stroke of this type of electrostatic actuation device; however, reference (2) incorporated the simple principle of the lever to increase the available stroke in the system at the expense of increasing the required voltage for actuation (Figure 2).

The vertical deflection of the structure shown in Figure 2 is limited by the thickness of the sacrificial oxide, which forms the electrostatic gap. The approach used in the SUMMiT™ pull down design of the programmable gratings utilizes a compound beam, which is enabled by the additional layers available within SUMMiT™. The available stroke in this case is the sum of the thicknesses of Sacox1, Sacox3, MMpoly1 and MMpoly2, which is 6.5 microns.

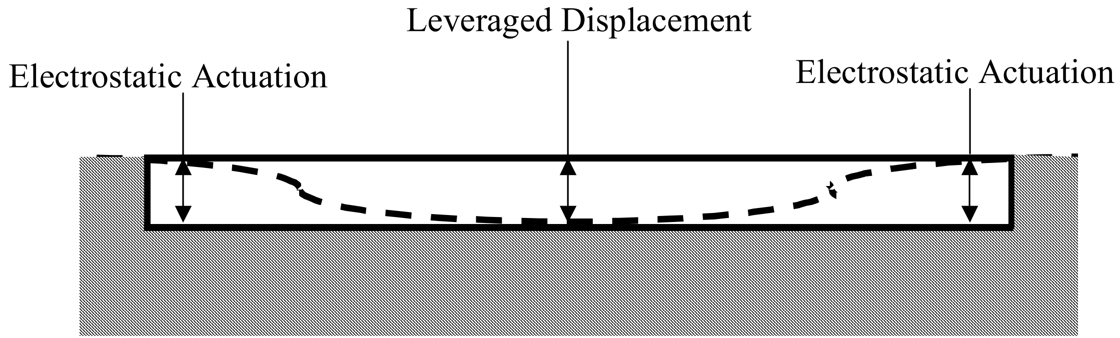

Figure 2. Schematic Representation of Leveraged Beam Bending.

Figure 3 shows a schematic view of the actuating beams in the SUMMiT™ implementation. There are actuation pads associated with both the MMPOLY2 beams (red) and the MMPOLY3 beam (blue). The MMPOLY2 beam that is 2 microns from the substrate will be electrostatically pulled down by the associated MMPOLY2 actuation pad until the MMPOLY2 touches the substrate. With appropriate sizing of the beam length and electrode pad length this can be accomplished without encountering the electrostatic-structural instability. This will also put the MMPOLY3 beam, which was originally 6.5 microns from the substrate closer, which enables large forces and greater additional vertical stroke. The MMPOLY3 actuation pads will then electrostatically pull the MMPOLY3 beam to the full deflection of 6.5 microns. Again, with appropriate sizing of the beam and electrode lengths this can be accomplished without encountering the electrostatic-structural instability.

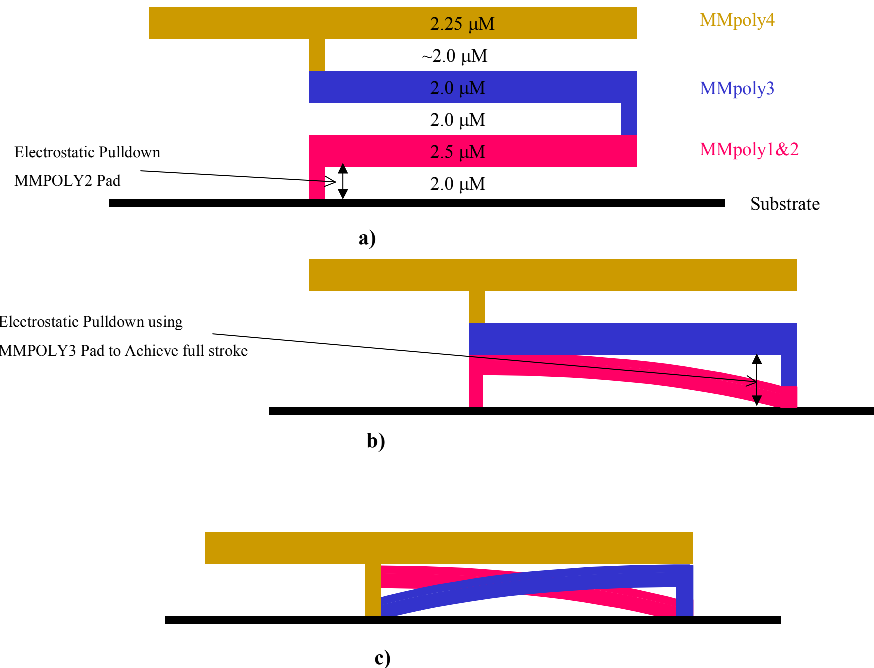

Figure 3. Schematic of Compound Beam Leveraged Bending Operation.

Figure 4 shows a solid model of the compound beam used in the leveraged bending. It can be seen that the MMPOLY2 and MMPOLY3 beams must be laterally offset to enable this design approach.

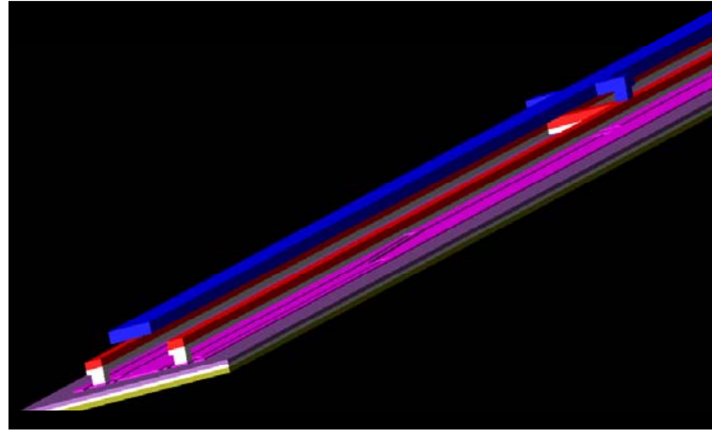

Figure 4. SUMMiT™ Implementation of the Leveraged Bending Design.

The use of a segmented design is required to minimize residual stress effects. There are various design perturbations in the ordering of the supports and segmentation of the actuating beams that have been investigated. In our pull down designs we are not relying on symmetry and the cyclic nature of a structure to enable adequate mirror flatness. The approach we used to minimize residual stress effects and enable the use of leveraged beam bending was the "Toadstool" design (Figure 5). This structure is symmetrical about the Poly2 anchor. Since there is only one anchor to the substrate the residual stress in the MMPOLY2 and MMPOLY3 beams will cancel out, leaving the structure minimally perturbed. In fact the "Toadstool" structure is only sensitive to the difference in residual stress in MMPOLY2 and MMPOLY3. Also since the MMPOLY4 mirror surface is attached only at one point, it is immune to average residual stress effects. Figure 5 is a side view of this design. The MMPOLY2 and MMPOLY3 beams are arranged as shown in Figures 6 and 7 for the "Toadstool" design. Figure 8 is an image of a small test array of devices fabricated in the SUMMiT™ process.

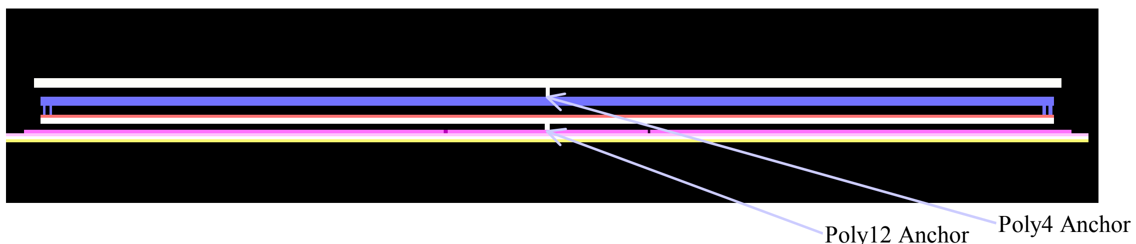

Figure 5. Side View of the "Toadstool" Segmented Programmable Grating.

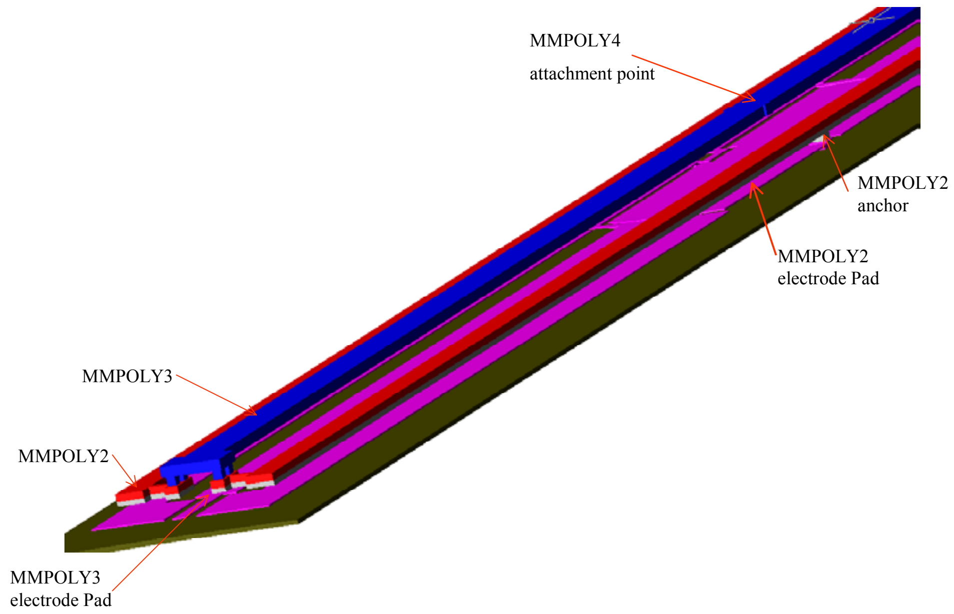

Figure 6. Isotropic View of the "Toadstool" Segmented Programmable Grating (MMPOLY4 not shown).

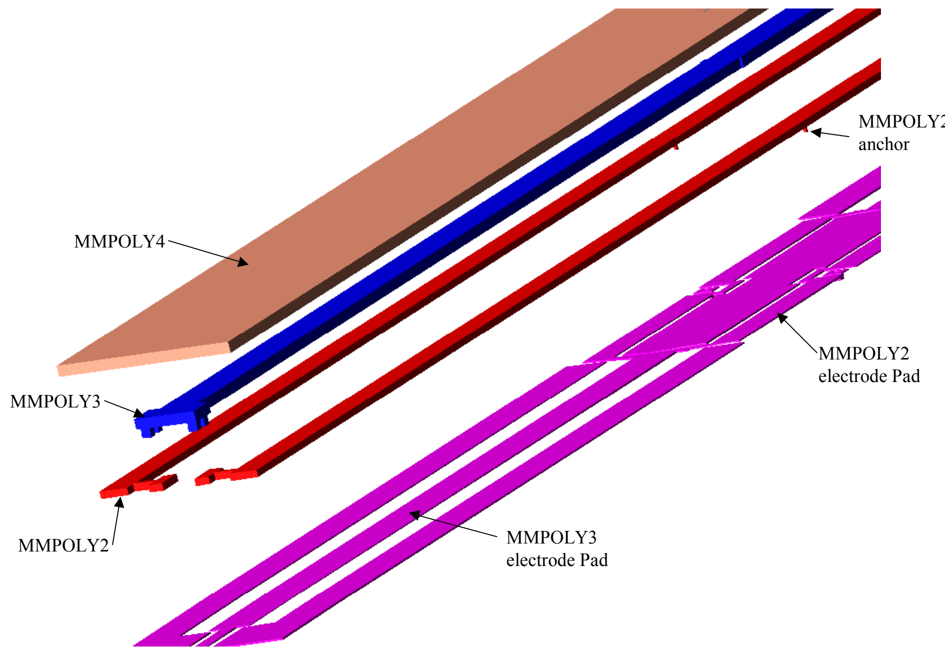

Figure 7. Exploded View of the "Toadstool" Segmented Programmable Grating.

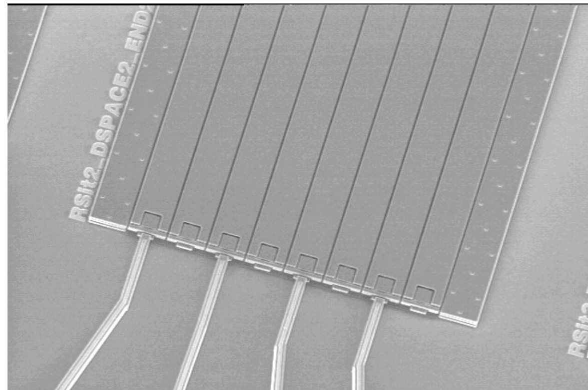

Figure 8. SUMMiT V™ Variable Programmable Grating Test Array.

The measured and analytical data for the MMPOLY4 mirror deflection in the "Toadstool" design are shown in Figure 9. The measured vertical deflections show a discontinuity in the deflection curve, which is due to the MMPOLY2 beam touching down. Full deflection of the MMPOLY2 beam is achieved without encountering electrostatic – structural instability. The MMPOLY3 beam was able to deflect an additional 0.7 microns before it encountered electrostatic – structural instability. Future designs will vary the beam and electrode lengths to achieve additional deflection.

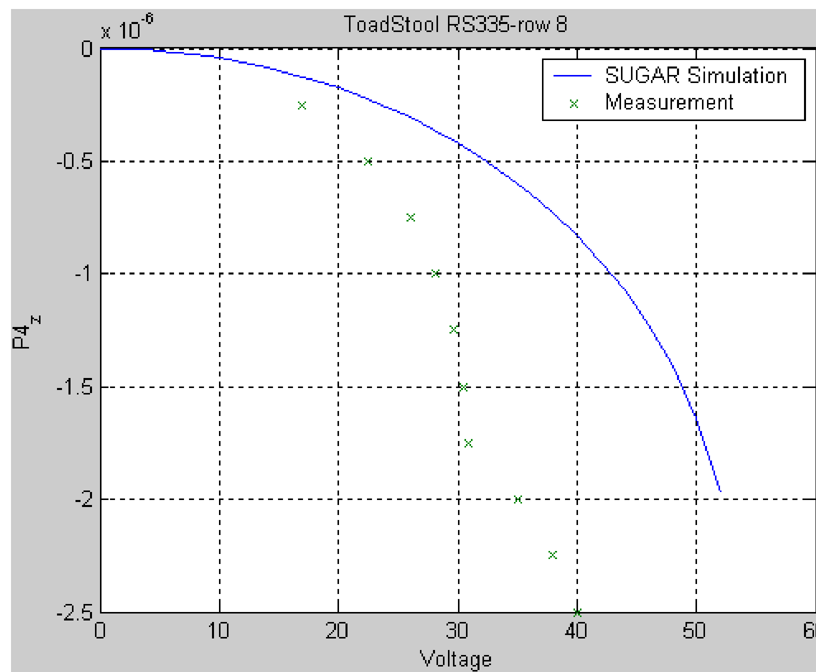

Figure 9. Voltage vs. Deflection of MMPOLY4 Mirror in the "Toadstool" Design.

Push-Up Programmable Grating Design

Designing a programmable grating to move up is an alternative approach to achieving the design criteria. The push-up programmable grating design is schematically shown in Figure 10. This approach involves a symmetrical arrangement of an electrostatically actuated lever arm. The two symmetric electrostatic levers are connected via a flexure and platform, which connects to the MMPOLY4 grating surface. The design illustrated in Figures 11 and 12 represents one of many possible implementations. Design variations involve the details of the flexure and pivot as well as the geometric positioning of the various components. A number of variations have been designed and are in the process of fabrication on SUMMiT™ reticle set 353, which is due for completion in November 2002.

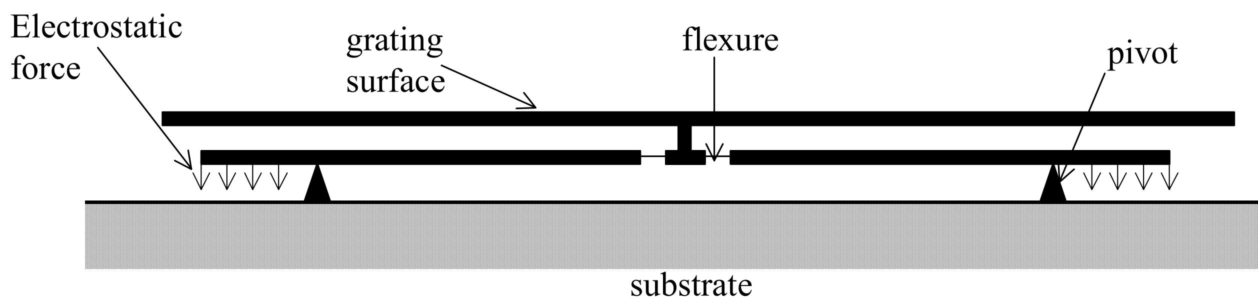

Figure 10. Schematic of the Push-Up Programmable Grating Design.

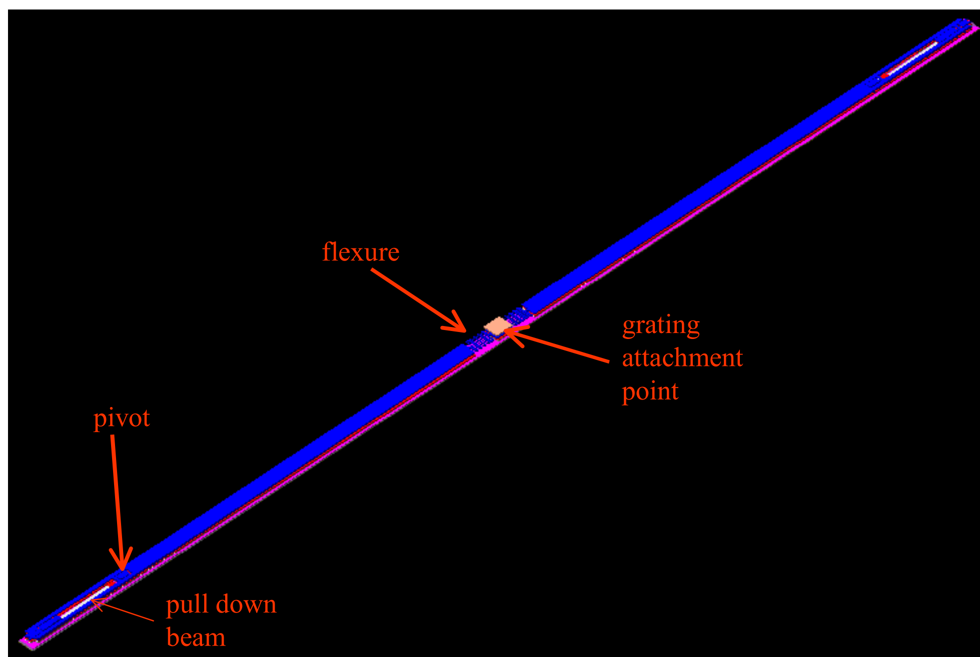

Figure 11. 3-D Model of the Push-Up Design (MMPOLY4 grating surface not shown).

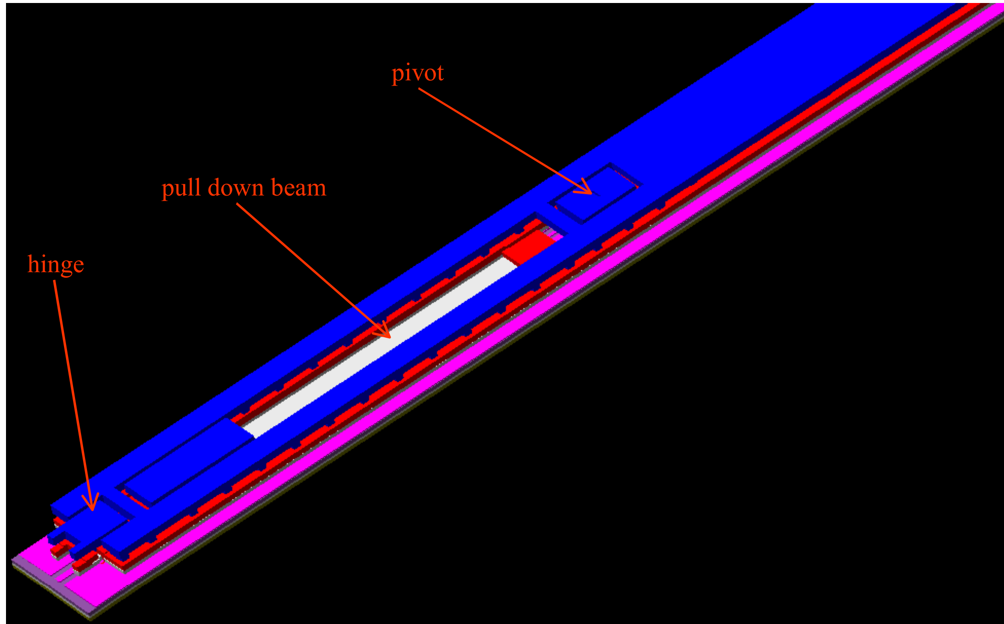

Figure 12. Detailed View of the Actuating Beam and Joints in the Push-Up Design.

The principal advantage of the push-up programmable grating is that the amount of vertical deflection attained by the design is not constrained by the thicknesses of the SUMMiT™ layers. This design approach is very simple to analyze and design.

Rotational Programmable Gratings

A rotational programmable grating that utilizes vertically interdigitated comb drives for actuation has been designed and fabricated. Figure 13 shows a solid model of the vertical comb drive rotational grating. Figure 14 is an image of the SUMMiT™ rotational programmable grating.

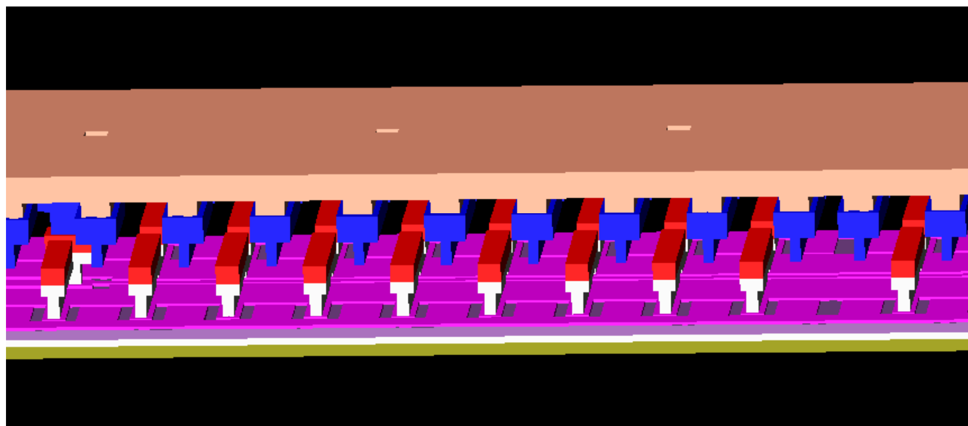

Figure 13. Solid Model of Rotational Programmable Grating.

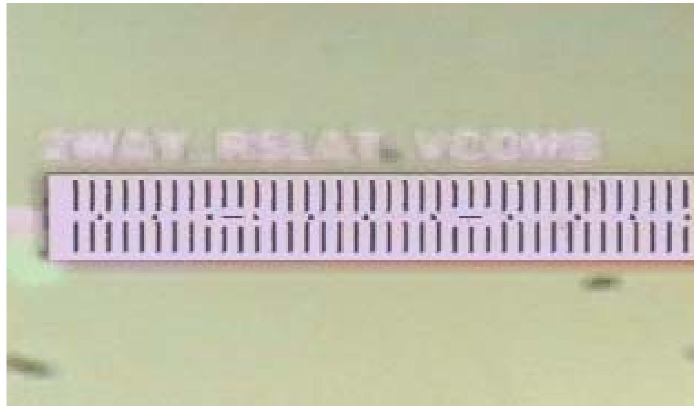

Figure 14. SUMMiT™ Rotational Programmable Grating.

Conclusions

The objective of this portion of the LDRD is to develop a variable programmable grating structure within the SUMMiT™ surface micromachining fabrication process that will be used in an optical chemical detection system. The variable programmable grating consists of an array of vertically actuated "slats," which can be actuated to mimic the spectrum of a particular chemical. This will be used as the reference cell in the correlation spectrometer dubbed the Polychromator.

The status of the SUMMiT™ Polychromator is as follows:

- Developed design concepts for programmable grating structures that have a combination of vertical and rotational degrees of freedom (DOF).
- Designed 4 sets of modules based upon these concepts (RS-331, RS-335, RS-353, RS 372) based upon these concepts.
- Two reticle sets have completed fabrication (RS-331,RS-335). Figures 8 and 14 show images of vertical and rotational programmable gratings from these reticle sets.
- Evaluated designs of structures that minimize residual stress effect. The "Toadstool" design appears to minimize the residual stress to an acceptable degree.

Preliminary design evaluation results have shown the following:

- A structure ("Toadstool") has been developed and successfully actuated that minimizes residual stress effects.
- "Toadstool" programmable grating achieved 2.5 microns of vertical stroke.
- Rotational degree of freedom programmable grating structures have been successfully actuated.

References

[1] M. B. Sinclair, M. A. Butler, S. H. Kravitz, W. J. Zubrzycki, A. J. Ricco, "Synthetic Infrared Spectra", *Optics Letters*, vol. **22**, no. 13, July 1, 1997.

[2] S. D. Senturia and E. S. Hung, "Extending the Travel Range of Analog-Tuned Electrostatic Actuators", *JMEMS*, vol. **8**, no. 4, December, 1999.

PART II

A Surface-Micromachined Microelectromechanical Encoding Mask for Hyperspectral Imaging

Daryl J. Dagel
MEMS Device Technologies

Olga Blum Spahn
RF Microsystems Technologies

Joe C. Wehlburg
Remote Sensing and Exploitation

Christine M. Wehlburg
Chemical and Biological Sensing, Imaging and Analysis

Sandia National Laboratories
P.O. Box 5800
Albuquerque, NM 87185

Abstract

First-generation mirror arrays targeted to replace the TI DMD™ in an infrared hyperspectral imager have been fabricated and tested. These Venetian Blind Mirrors (VBMs) are long and narrow mirrors and tilt back and forth when voltage is applied to their underlying electrodes. Operation voltages exceed 100 V as a result of their highly rectangular geometry and lead to electrical failure when fully tilted. This insight is being used to redesign the mirrors with reduced actuation voltages and with larger minimum separations. The potential advantages of these VBMs are optical in nature: better match to the diffracted light, fewer gaps between mirrors, smoother surface profile, and higher reflectivity. Together they translate into improved signal-to-noise, which will enhance the identification capability of the hyperspectral imager.

Table of Contents

Abstract…… 20
Table of Contents…… 21
List of Figures…… 21
List of Tables…… 21
Introduction…… 22
MEM Spectral Encoding Mask…… 22
Venetian Blind Micro-Mirrors…… 24
Results and Discussion…… 25
Conclusions and Future Work…… 29
References…… 30

List of Figures

Figure 1: Hadamard Transform Spectral Imager (HTSI)…… 23
Figure 2: Schematic of Venetian Blind Mirror (VBM)…… 24
Figure 3: Cross-Section of 50×1000 μm^2 VBM…… 25
Figure 4: Video Microscope Image of Fabricated VBM Arrays…… 26
Figure 5: White-Light Interferogram of 50×1000 μm^2 Mirrors…… 26
Figure 6: White-Light Interferogram of Tilted VBM…… 27
Figure 7: Simulated and Measured Voltage Response of 50×1000 μm^2 Mirrors…… 27
Figure 8: SEM of Electrode after ESD Breakdown…… 28
Figure 9: Video Microscope Image of Dimple Debris…… 29

List of Tables

Table 1: Target Specifications for MEM Encoding Mask…… 23
Table 2: Mirror Array Parameters for VBMs…… 25

Introduction

Hyperspectral imaging is a powerful tool for remote sensing. By sampling hundreds of narrow, contiguous wavelength bands, the characteristic reflectance spectra of many objects can be identified and used to determine the composition of an area in great detail. This technique represents the state-of-the-art in imaging spectroscopy and finds broad application in scientific studies of the environment (crops, vegetation, rocks, minerals) as well as in military reconnaissance and monitoring.

A number of devices exist for sampling visible and infrared spectra, for example, slit scanning and Fourier transform spectrometers. The hyperspectral device described here utilizes the Hadamard transforming technique to achieve a greater signal-to-noise ratio than simple slit-scanning techniques [1]. In the Hadamard approach a predetermined subset of the source spectrum is sampled for detection, and the measurement is repeated for many different subsets. By inverting the matrix of intensities from all of these subsets, the individual wavelength components can be recovered and analyzed.

A schematic of the Hadamard Transform Spectral Imager (HTSI) in its current configuration appears in Figure 1 [1]. The imager consists of five basic components: (1) a diffraction grating, which spatially separates the source spectrum into its constitutive wavelengths; (2) a micro-mirror array (Texas Instruments DMD™), whose elements selectively reflect the dispersed light into and out of the optical system; (3) a second grating, which recombines the reflected light from the DMD™; (4) a 2D detector for simultaneous measurement of the encoded image; and, (5) a computer for controlling the DMD™ and for processing the detector signals in real time.

The benefits of the HTSI include variable spectral and temporal resolution, insensitivity to vibration, and lack of moving parts, other than the simple back and forth tilting of the micro-mirrors.

MEM Spectral Encoding Mask

The TI DMD™ lies at the heart of the HTSI and serves as the one-dimensional spectral encoding mask for image processing. Not surprisingly, the DMD™ has some disadvantages for this application, considering that it was designed to operate as a two-dimensional spatial mask for visible light [2]. First, the DMD™ mirrors are square and tilt on a diagonal. The ideal shape for mirror elements in the HTSI is the highly rectangular geometry possessed by the wavelength bands coming from the diffraction grating. This requires that several square mirrors be electrically connected to form a single reflective "slat." Gaps between the mirrors generate unwanted diffraction, and diagonal tilting results in a jagged reflective surface rather than an ideal rectangular one. In addition, large anchor depressions in the middle of each mirror generate additional noise and loss. Moreover, the reflectivity of the aluminum mirrors is not optimized for the wavelength range of interest (the infrared region between 1.25 and 2.5 μm).

The goal of this project is to develop a replacement micro-mirror array that largely overcomes the limitations and drawbacks of the DMD™. The target specifications for this custom mirror array appear in Table 1. Given the stringent design goals, the only fabrication approach currently viable is surface micromachining, namely SUMMiT V™, Sandia's Ultra-planar Multi-level MEMS Technology.

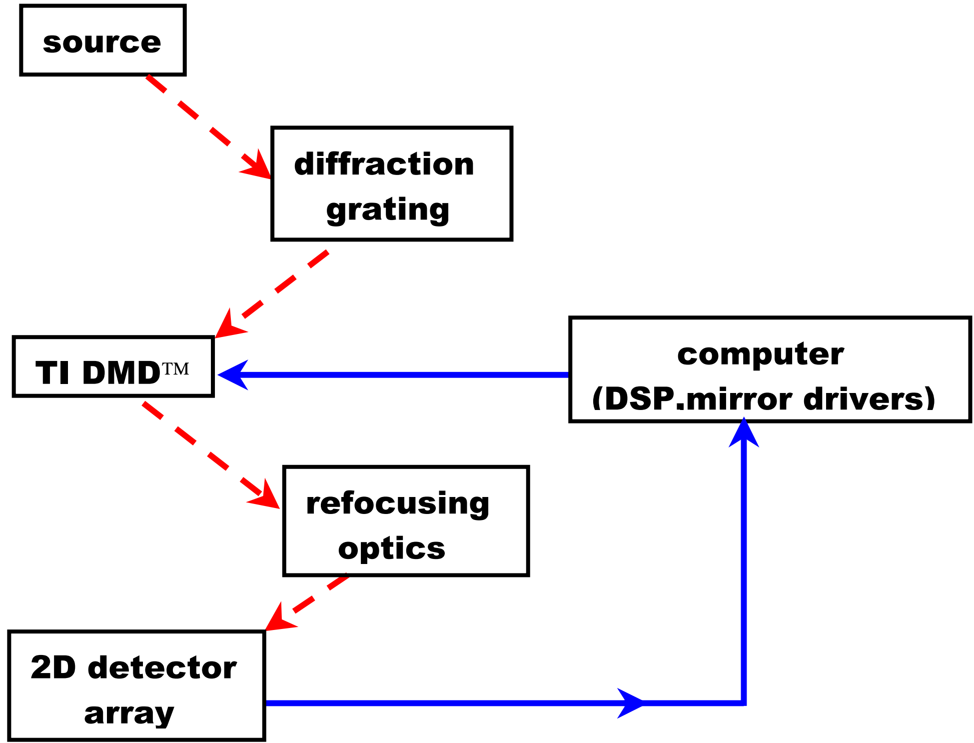

Figure 1. Hadamard Transform Spectral Imager (HTSI)

Table 1. Target Specifications for MEM Encoding Mask

operating environment	space satellite
operating wavelength	infrared (1.25 – 2.5 μm)
mirror size	30 – 60 × 1000 μm^2
array size	800 elements
angular rotation	±10°
switching speed	< 250 μs
switching voltage	< 150V (28 V standard)
fill factor	> 96%
Reflectivity	> 98%
mirror flatness	λ/20

SUMMiT V™ is the most advanced surface-micromachining process in the world and has been used extensively in the development of complex actuators and sensors [3]. The process consists of five polysilicon layers (poly0, poly1, poly2, poly3, and poly4) and four silicon dioxide layers (sacox1, sacox2, sacox3, and sacox4) alternately stacked like the layers of a cake. Polysilicon serves as a structural material because of its excellent mechanical and electrical properties, while silicon dioxide acts as a sacrificial material that is etched away during chemical release of the polysilicon structures. A thin layer of silicon nitride isolates the structures from the silicon substrate. In addition, two intermediate chemical-mechanical polishing (CMP) steps virtually eliminate conformal topography.

Venetian Blind Micro-Mirrors

As an initial design concept, straightforward tilting mirrors with electrostatic actuators were prototyped. A schematic of one of these mirrors, referred to as Venetian Blind Mirrors or VBMs, appears in Figure 2. They consist of a rectangular mirror plate supported by torsional springs on both ends, a pair of electrodes underneath the mirror, and a set of interstitial standoffs on which the mirror lands when fully tilted. Given the relatively long mirror length (1 mm), dimples and posts were inserted along the pivot axis to prevent the mirror from being simply pulled straight down and shorted to the electrodes. Figure 3 shows these design features in cross-section.

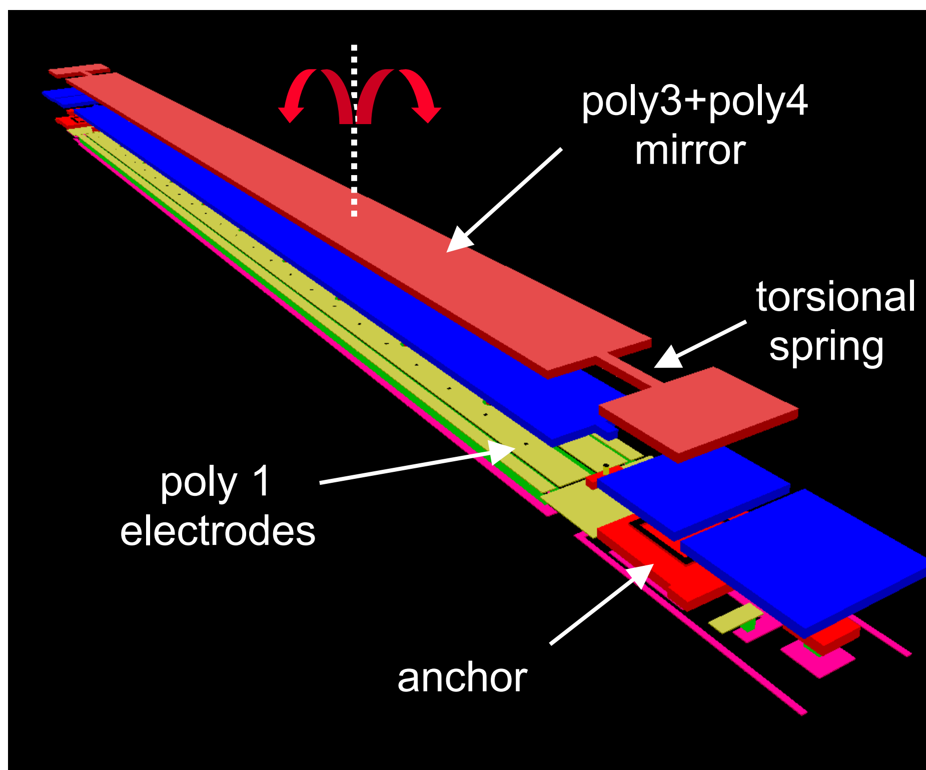

Figure 2. Schematic of Venetian Blind Mirror (VBM)

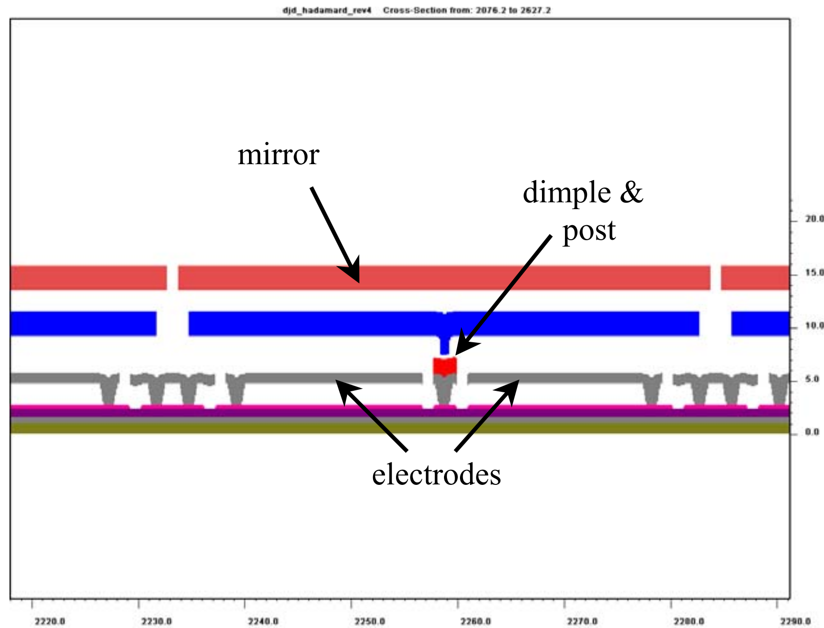

Figure 3. Cross-Section of 50×1000 μm² VBM

Three basic VBMs were investigated in the first fabrication run (reticle set RS331), the relevant parameters of which are listed in Table 2. The complexity and flexibility of SUMMiT V™ permit several of the target specs for these mirrors to be addressed simultaneously. For example, the availability of five polysilicon layers allows for reinforced mirrors, a critical feature in preventing stress-induced buckling when dealing with large MEMS structures (>250 μm). Also, by eliminating conformal topography, CMP produces an optically flat mirror surface.

Table 2. Mirror Array Parameters for VBMs

array size (mm²)	mirror size (μm²)	angular states (°)	switch voltage (V)	mirror spacing (μm)
0.5 × 1.0	30 × 1000	± 13.4	287	1
0.5 × 1.0	50 × 1000	± 7.5	103	1
0.5 × 1.0	30 × 1000	0, 9.1	144	1

Results and Discussion

An aerial view of one of the fabricated modules appears in Figure 4. Polysilicon wires connect the electrodes to bond pads located around the module periphery. The size and spacing of the bond pads facilitate wire bonding to a ceramic dip package. Before use in the HTSI, a thin film of gold (~1000 Å) must be evaporated on the mirrors to increase their reflectivity above

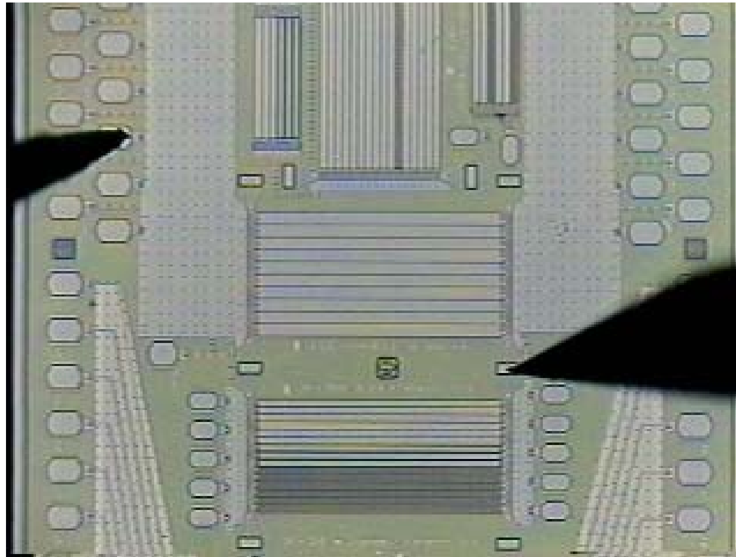

Figure 4. Video Microscope Image of Fabricated VBM Arrays.

97% in the infrared. A protective shield or shadow mask covers the wiring so that the gold can be deposited over the entire module without shorting out individual mirrors.

Several 50×1000 μm^2 mirrors were examined to determine their static surface topography. Figure 5 is a white-light interferogram of a portion of one array as fabricated. Stress-induced curvature from these VBMs was measured to be ~20 nm peak-to-valley, which far exceeds the $\lambda/20$ goal for the hyperspectral imager. The excellent mirror flatness can be attributed to the inherent low stress in the SUMMiT V™ polysilicon layers as well as to the rigid two-layer mirror structure.

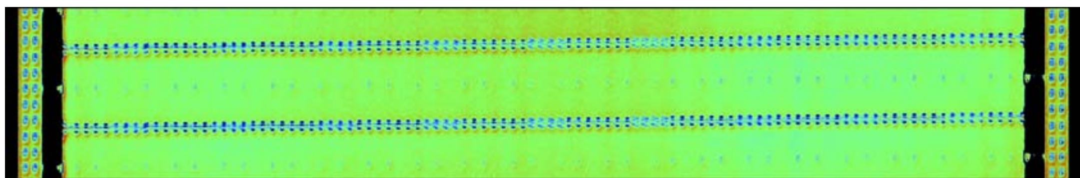

Figure 5. White-Light Interferogram of 50×1000 μm^2 Mirrors.

Electrostatic deflection profiles were measured in a similar way, and Figure 6 shows a close-up image of a slat tilted to 2.8° by a 130V dc voltage. A Matlab® program was developed to numerically solve the governing differential equation of the torsional mirror system [4]. This simulation predicts a voltage response typical of electrostatic actuators: a quadratic deflection region corresponding to the V^2 dependence of the force followed by an abrupt pull-in or snap-through to the electrode, or in this case, to a electrically grounded standoff.

Figure 7 compares the simulated behavior of a 50×1000 μm^2 slat with the experimentally measured data. As apparent from the figure, the simulated curve agrees well with the measured data when the air gap is set to 3.5 ± 0.1 microns. However, based on the SUMMiT V™ process

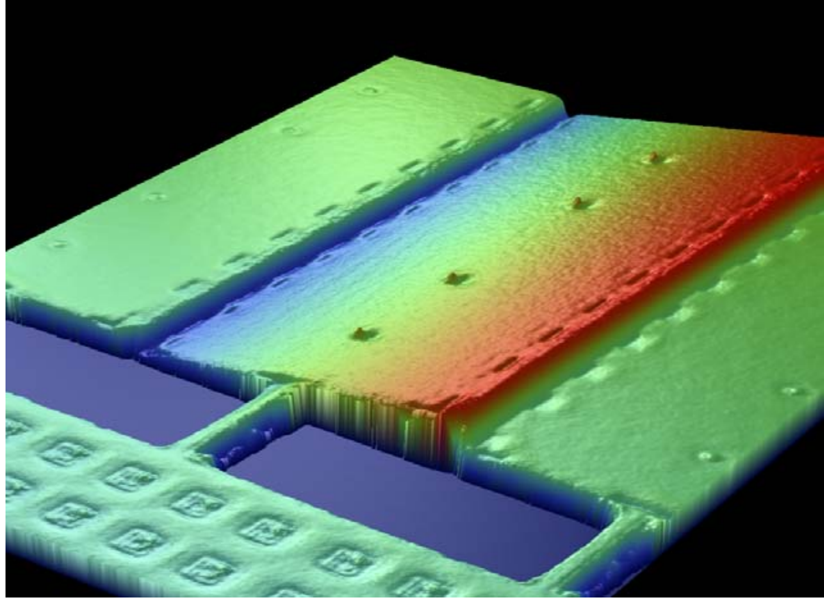

Figure 6. White-Light Interferogram of Tilted VBM.

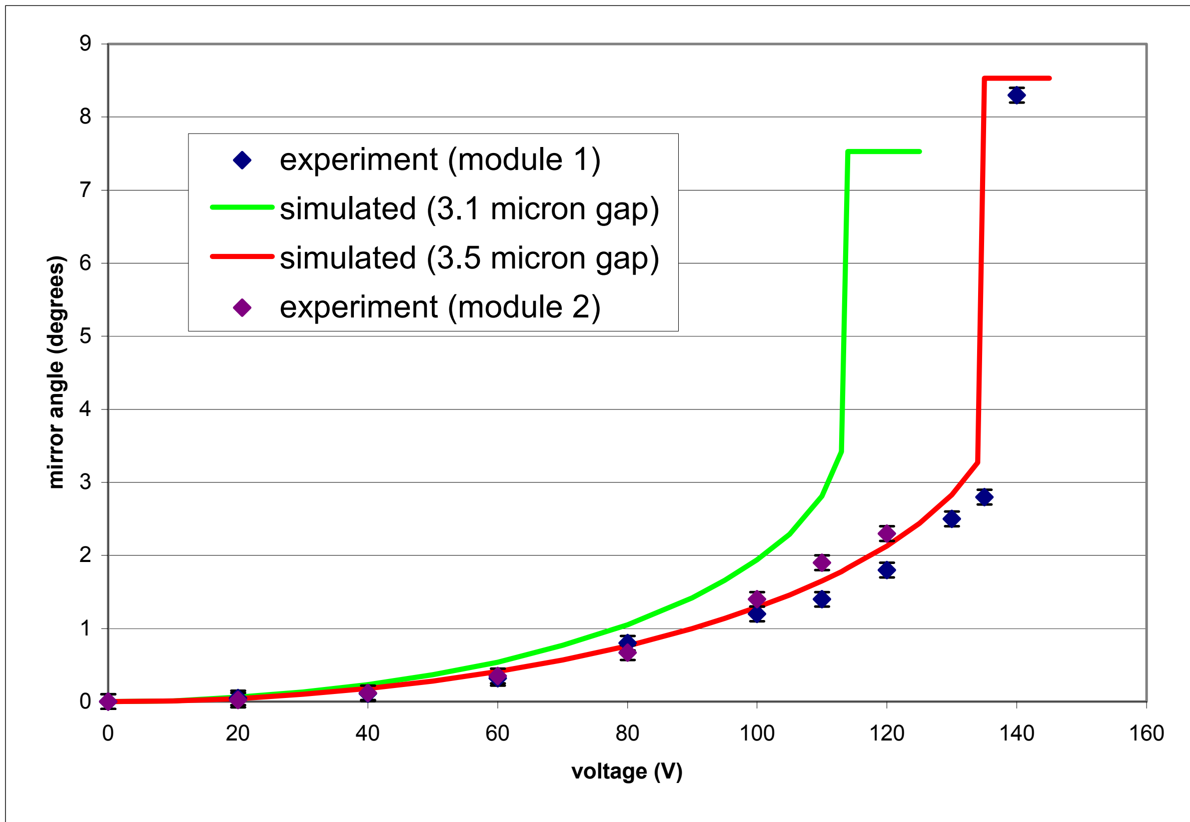

Figure 7. Simulated and Measured Voltage Response of 50×1000 μm^2 Mirrors.

parameters, the initial air gap between the mirror and the underlying electrode should be 3.1 ± 0.1 microns. This unexpected result was investigated through interferometric measurements of the polysilicon layer heights, which confirmed that the oxide (air gap after release) in question (sacox3) is ~0.6 μm thicker than expected.

As expected, pull-in occurs around 140V for the 50×1000 μm^2 VBMs. Angular repeatability could not be measured because the mirrors short out immediately after pull-in. Two corresponding failure modes have been identified: (1) electrostatic discharge (ESD) breakdown between the mirror and the electrode when the mirror is fully tilted, and (2) current or bending-induced dimple fracture. In the first scenario, the mirrors remain tilted even after the voltage is turned off, indicating that fusion between mirror and electrode has occurred. This ESD damage can be clearly seen in the scanning electron micrograph (SEM) of Figure 8 and has been attributed to field emission around surface asperities in similar studies [5].

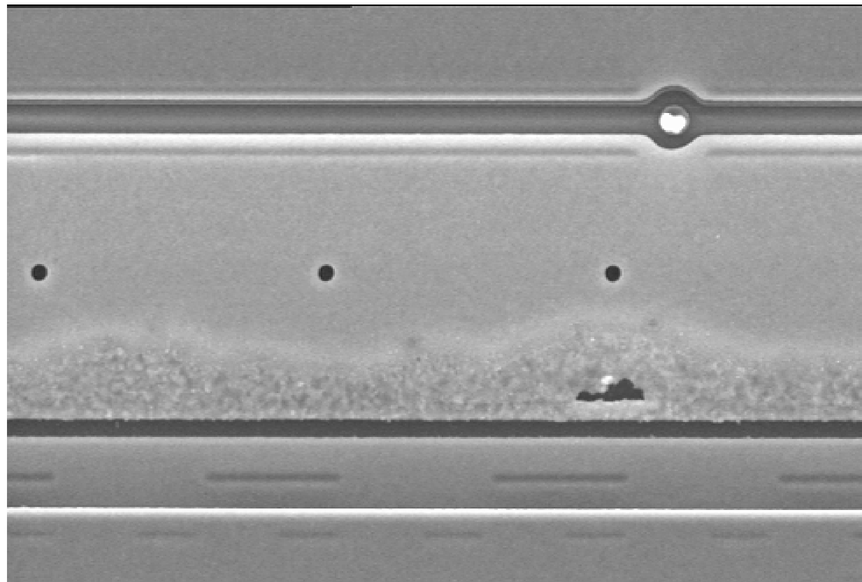

Figure 8. SEM of Electrode After ESD Breakdown.

In the second failure mode, the mirrors pop back to close to their original position after pull-in and can be actuated to at most 40V before shorting again. It is believed that in this case the dimple supports underneath the mirror break off and either energize the opposite electrode or short the powered electrode or both. Figure 9 shows such dimple debris and explains why the damaged slats can handle no more than 40V. What causes the dimples to fracture in the first place is not precisely clear, but two likely sources are the violence of pull-in itself and the electrical current resulting from unintended contact. Indeed, a small amount of buckling has been observed in these mirrors, suggesting that plastic deformation has occurred.

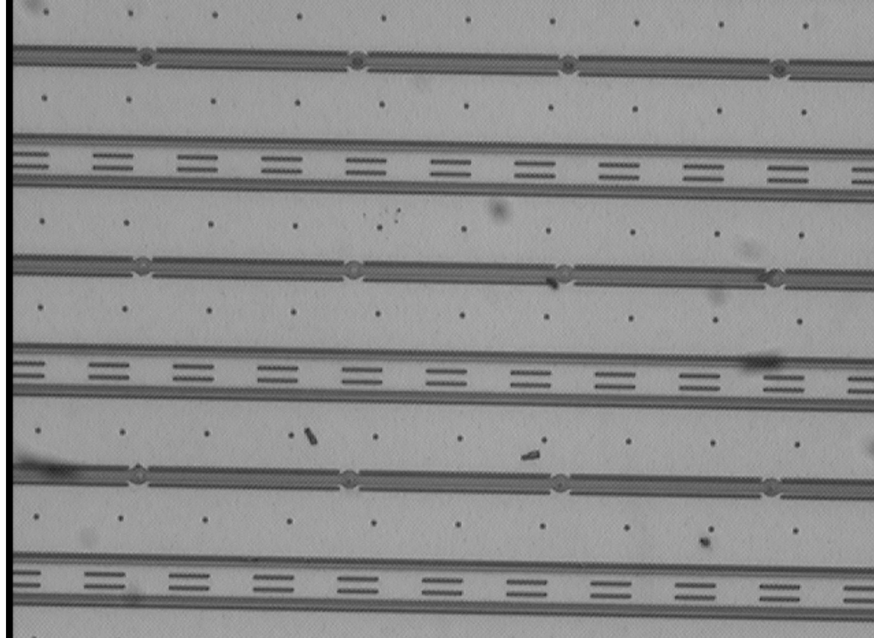

Figure 9. Video Microscope Image of Dimple Debris.

Conclusions and Future Work

First-generation mirror arrays targeted to replace the TI DMD™ in a Hadamard transform spectral imager have been designed, fabricated, and tested. Actuation voltages exceed 100 V due to the constrained lateral geometry of the mirror elements and results in catastrophic failure at large tilt angles. Further investigation of the breakdown behavior between two polysilicon films at narrow separations (< 5 μm) needs to be done.

The potential advantages of the Venetian Blind Mirrors are optical in nature: better match to the diffracted light, fewer gaps between mirrors, smoother surface profile, and higher reflectivity. Together they translate into improved signal-to-noise, which will enhance the identification capability of the hyperspectral imager. Current work focuses on modeling the coupled electro-mechanical deflection of the VBMs using finite-element analysis (FEA) and on making design modifications that avoid electrical breakdown by substantially reducing the pull-in voltage and by increasing the minimum air gaps. High-speed photography is also being used to quantify switching speed and dynamic behavior.

References

[1] C.M. Wehlburg, J.C. Wehlburg, S.M. Gentry, and J. Smith, "Optimization and Characterization of an Imaging Hadamard Spectrometer," *Proc. SPIE*, vol. **4381**, pp. 506-515, 2001.

[2] http://www.dlp.com/

[3] http://www.sandia.gov/mstc/

[4] M.-H. Kiang, O. Solgaard, K.Y. Lau, and R.S. Muller, "Electrostatic combdrive-actuated micromirrors for laser-beam scanning and positioning," *J. Microelectromech. Syst.*, vol. **7**, no. 1, pp. 43-47, 1998.

[5] R.M. Schaffert, *Electrophotography*, chp. **4**, The Focal Press, New York, 1965.

Distribution List

1	MS0188	D.L. Chavez, LDRD Office
1	MS0603	C.T. Sullivan, 1742
1	MS0603	O.B. Spahn, 1742
1	MS0603	F.R. Gass, 1742
1	MS0603	G.D. Grossetete, 1742
1	MS0886	C.M. Wehlburg, 1812
1	MS0972	J.C. Wehlburg, 5712
1	MS1080	D.R. Sandison, 1769
3	MS1080	J.J. Allen, 1769
3	MS1080	D.J. Dagel, 1769
1	MS1080	J.L. Dohner, 1769
1	MS1080	S.S. Mani, 1749
1	MS1411	M.B. Sinclair, 1851
1	MS1425	K.B. Pfeifer, 1744
1	MS9018	Central Technical Files, 8945-1
2	MS0899	Technical Library, 9616
1	MS0612	Review & Approval Desk, 9612